

## Angular Momentum Control for Preventing Rollover of a Heavy Vehicle

Faruk Ünker<sup>1\*</sup>

0000-0002-9709-321X<sup>1</sup>

<sup>1</sup>Mechanical Engineering Department, Gümüşhane University, Gümüşhane, 29100, Türkiye

### Abstract

In this article, gyroscopes and flywheels are used to prevent the rollover of a vehicle due to external forces. The rollover preventing performance of the flywheels for a heavy trailer (an inverted pendulum problem) is investigated at a high road bank angle risk. Two control moment gyroscopes (CMG) and a reaction wheel are controlled by proportional torques to keep the vehicle in a stable motion in the vertical position. The reaction wheel was used only to eliminate the dissipation energy of damper. By using the energy stored in the flywheels of gyroscopes, the sprung mass of a vehicle can make a stable oscillating motion of small amplitude, standing upright without tipping over. The optimum flywheel speed was derived from the frequency equations with the appropriate controller gain. Most importantly, the required angular momentum to keep the vehicle upright without tipping over depends on the amplitude of the gimbal oscillation and the frequency. It has also been observed that Matlab simulations of Lagrangian equations and simulations modeled in RecurDyn software are in perfect harmony.

**Keywords:** Active control; Angular momentum; Gyrostabilizer; Flywheel; Reaction wheel; Vehicle

### Research Article

<https://doi.org/10.30939/ijastech..1085111>

Received 09.03.2022  
Revised 17.05.2022  
Accepted 10.06.2022

\* Corresponding author

Faruk Ünker

[farukunker@gumushane.edu.tr](mailto:farukunker@gumushane.edu.tr)

Address: Mechanical Engineering Department, Faculty of Engineering and Natural Sciences, Gümüşhane University, Gümüşhane, Türkiye  
Tel: +904562331000

## 1. Introduction

Owing to the serious safety issue of the high center of gravity, a rollover can cause dangerous accidents for commercial or sport utility vehicles. Many rollover control systems for these vehicles have been proposed in recent years [1–3]. Besides, the road angle is an important factor in rollover. The static rollover stability is controlled through increasing of the vehicle's geometric roll resistance. However, this geometric roll design might not be adequate in height of the center of gravity (CG) vehicles such as trucks. Therefore, angular momentum of a flywheel can be used as a direct roll control technique for stabilization of roll motion instead of increasing of the vehicle's geometric roll resistance [4,5]. Therefore, consisting of CMG can perfectly provide the stability of an inverted pendulum-like high CG vehicles [5].

This article introduces a new rollover controller method that utilizes the rotational kinetic energies of the flywheels to stabilize a heavy vehicle under continuous load in the direction of gravity. The rollover preventing the performance of the flywheels for a heavy trailer (an inverted pendulum problem) is investigated at a high road bank angle risk. Flywheels can provide motion control at broadband excitation frequencies because the flywheel speed can exert counter-thrust on any vehicle that can overcome destabi-

lizing forces [6,7]. Recently, various studies based on the gyroscopic moment of inertia of a rotating flywheel have eliminated unwanted movements on structures by various methods [5–7]. The kinetic energy of a flywheel stabilizer offers weight and volume savings and an unresponsive ride compared to conventional anti-roll controllers [5,7]. The oscillating motion of the gimbal keeps the mass of the vehicle in stable constant periodic motion in the upright position [5]. Therefore, the angular momentum of a flywheel can stabilize vehicles against constant forces.

## 2. Model Setup

The flywheels can rotate freely around the axis of rotation inside the gimbals mounted under the trailer as shown in Figures 1-3. The numerical characteristics of the vehicle model and stabilizers used in the study are shown in Table 1. To ignore the unwanted reaction torques, the vehicle is composed of two gyroscopic flywheels and a reaction wheel. The reaction wheel is assumed to have a rotational speed  $\dot{\psi}$  against damping torque ( $c\dot{\psi}$ ) whilst gyroscopes' flywheels move in opposite orientations to each other to maintain the sprung mass in a stable upright position. The road bank angle,  $\alpha$  is excited to the axle of the trailer having stiffness ( $k$ ) and damping ( $c$ ) in torsional along the roll direction as seen in Figure 4. In the vehicle, the precession of a gimbal is used as the proportional

input control,  $P$  whilst the output control is the torque to remain the gimbal stable as shown in Figure 5. Besides, the reaction wheel is controlled by an acceleration to eliminate the damping torque for sprung stability taking the sprung's rollover velocity as the input of the controller.

Table 1. Model parameters of the physical system.

Gravity acceleration ( $m/s^2$ )	9.80665
Mass centroid length of the sprung (m)	1.786
Sprung mass (kg)	13663.869
Reaction wheel's rotary inertia ( $kg.m^2$ )	58.128
Flywheel's rotary inertia of gyroscope, ( $kg.m^2$ )	58.128
Flywheel's inertia of gyroscope ( $kg.m^2$ )	30.822
Gimbal's principal moment inertia of gyroscope ( $kg.m^2$ )	20.255
Gimbal's moment inertia of gyroscope, ( $kg.m^2$ )	19.633
Gimbal's moments inertia of gyroscope ( $kg.m^2$ )	2.461
Gimbal's mass moment inertia of reaction wheel ( $kg.m^2$ )	19.633
Mass inertia of the sprung ( $kg.m^2$ )	16099.476
Rotating speed of each gyroscope's flywheel (rad/s)	180-1689
Road bank angle (rad)	$\pi/8$
Equivalent stiffness coefficient of suspensions against rotation. (N.m/rad)	25000
Equivalent damping coefficient of suspensions against rotation. (N.m.s/rad)	10000

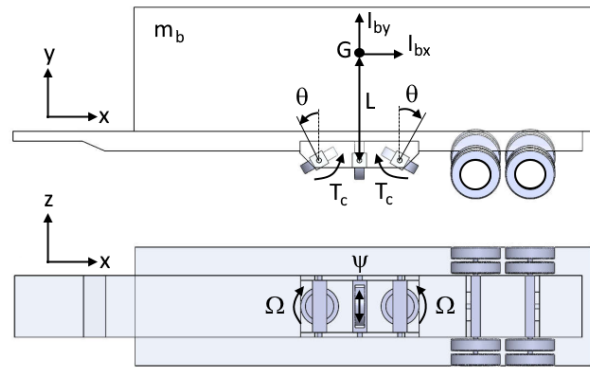


Fig. 2. Reaction wheel and gyros in sprung with the centroid (G)

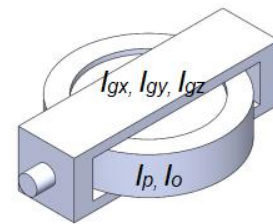


Fig.3. Gyroscope with the inertias ( $I_{gx}, I_{gy}, I_{gz}, I_p, I_o$ )

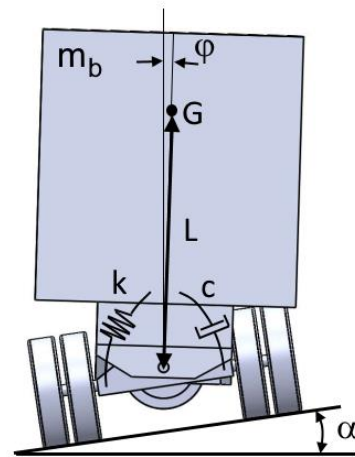


Fig. 4. Rollover position of vehicle, joining a suspension

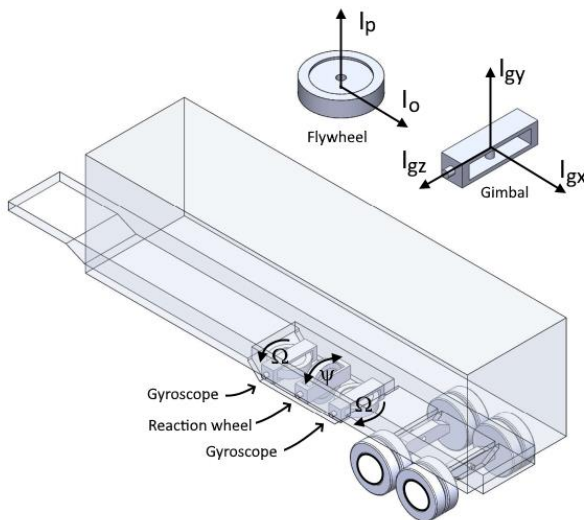


Fig. 1. Trailer model with gyros and reaction wheel

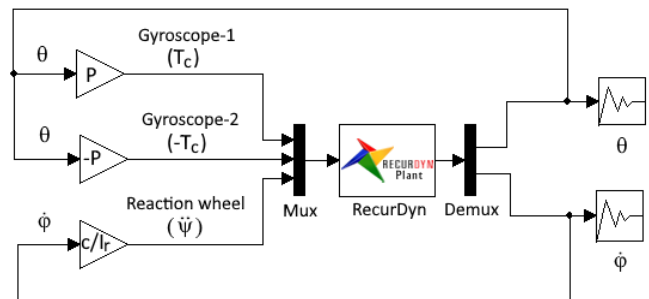


Fig. 5. Controller schematic diagram

### 3. Motion Equations and Derivation of Relations

A trailer sprung mass with two gyroscopes and the reaction wheel is given in Figures 1 and 2. To obtain the kinetic energy of the whole system, let us write the kinetic energy of each part of the model as follows.

$$T_{gyroscope} = \frac{1}{2}I_o[\dot{\theta}^2 + (\dot{\varphi} \cos \theta)^2] + \frac{1}{2}I_p(\Omega + \dot{\varphi} \sin \theta)^2 + \frac{1}{2}I_{gx}(\dot{\varphi} \cos \theta)^2 + \frac{1}{2}I_{gy}(\dot{\varphi} \sin \theta)^2 + \frac{1}{2}I_{gz}\dot{\theta}^2; \quad (1)$$

$$T_{reaction\ wheel} = \frac{1}{2}I_r(\dot{\psi} + \dot{\varphi})^2 + \frac{1}{2}I_y\dot{\varphi}^2; \quad (2)$$

$$T_{sprung\ mass} = \frac{1}{2}m_b[(L\dot{\varphi} \sin \varphi)^2 + (L\dot{\varphi} \cos \varphi)^2] + \frac{1}{2}I_{bx}\dot{\varphi}^2. \quad (3)$$

Therefore, the total energy of the stabilizers and trailer can be given as follows:

$$T_{total} = 2T_{gyroscope} + T_{reaction\ wheel} + T_{sprung\ mass}. \quad (4)$$

Flywheels and gimbals are placed in the sprung rotation center for the minimum potential energy of the trailer as stated below.

$$V = m_b g L \cos \varphi + \frac{1}{\alpha} k (\varphi - \alpha)^2. \quad (5)$$

Dissipation energy (D) is as seen in Equation (6):

$$D = \frac{1}{\gamma} c (\dot{\varphi} - \dot{\alpha})^2. \quad (6)$$

The equations of motion of the trailer model can be obtained by the Lagrangian method with the help of the following equations:

$$\frac{d}{dt} \left( \frac{\partial T_{total}}{\partial \dot{\theta}} \right) - \frac{\partial T_{total}}{\partial \theta} + \frac{\partial D}{\partial \dot{\theta}} + \frac{\partial V}{\partial \theta} = 2T_c; \quad (7)$$

$$\frac{d}{dt} \left( \frac{\partial T_{total}}{\partial \dot{\varphi}} \right) - \frac{\partial T_{total}}{\partial \varphi} + \frac{\partial D}{\partial \dot{\varphi}} + \frac{\partial V}{\partial \varphi} = 0. \quad (8)$$

Thus, the differential Lagrangian equations representing the motions of the vehicle are obtained as follows:

$$(I_o + I_{gz})\ddot{\theta} + (I_o - I_p + I_{gx} - I_{gy})\dot{\varphi}^2 \cos \theta \sin \theta - I_p \Omega \dot{\varphi} \cos \theta = T_c; \quad (9)$$

$$(2I_o \cos^2 \theta + 2I_p \sin^2 \theta + 2I_{gx} \cos^2 \theta + 2I_{gy} \sin^2 \theta + I_r + I_{bx} + I_y + m_b L^2)\ddot{\varphi} + 4(I_p - I_o + I_{gy} - I_{gx})\dot{\varphi} \dot{\theta} \sin \theta \cos \theta + 2I_p \Omega \dot{\theta} \cos \theta - m_b g L \sin \varphi + c(\dot{\varphi} - \dot{\alpha}) + k(\varphi - \alpha) + I_r \dot{\psi} = 0; \quad (10)$$

### 3.1 Amplitudes and Flywheel Speed Derived from Reduced Equations

For the zero amplitude ( $\varphi \approx 0$ ,  $\sin \varphi = \varphi$  and  $\cos \varphi = 1$ ) oscillation of the trailer, suppose that the acceleration of the rolling motion of the trailer at the equilibrium point of oscillation has a value so small that it can be neglected ( $\ddot{\varphi} \approx 0$ ) at the constant road bank angle. Also, the gimbal's kinetic energy is zero when it has zero precession in its approximate equilibrium position ( $\theta \approx 0$ ,  $\sin \theta = \theta$ , and  $\cos \theta = 1$ ). Therefore, the higher power velocity terms ( $\dot{\varphi} \approx 0$  and  $\dot{\theta} \approx 0$ ) for the balance point at approximately zero angle for the gimbal can be neglected. After that, Equations (9) and (10) are simplified by using these assumptions in the differential motion equations of the mathematical model as follows:

$$(I_o + I_{gz})\ddot{\theta} - I_p \Omega \dot{\varphi} = T_c; \quad (11)$$

$$2I_p \Omega \dot{\theta} - m_b g L \varphi + c \dot{\varphi} + k \varphi = k \alpha - I_r \dot{\psi}. \quad (12)$$

Let's assume that the following harmonic movements must occur to prevent the rollover caused by the gravitational force acting on the center of gravity of the trailer (5).

$$\theta(t) = -\theta_0 \sin(\omega t); \quad (13)$$

$$\varphi(t) = \varphi_0 [1 - \cos(\omega t)]. \quad (14)$$

To obtain a small roll vibration ( $\varphi_0 \approx 0$  and  $\cos \varphi_0 = 1$  and  $\sin \varphi_0 = \varphi_0$ ) Equations (11) and (12) can be reduced into the following form for  $\tau = -I_r \dot{\psi} = c \dot{\varphi}$  and  $T_c = P \theta$ ;

$$(I_o + I_{gz})\omega^2 \theta_0 - I_p \Omega \omega \varphi_0 = -P \theta_0 \quad (15)$$

$$-2I_p \Omega \omega \theta_0 \cos(\omega t) - m_b g L \varphi_0 [1 - \cos(\omega t)] + k \varphi_0 [1 - \cos(\omega t)] = k \alpha. \quad (16)$$

Hereby, one can obtain the the gimbal's, the sprung's roll amplitudes, and the frequency by solving above equations as follows

$$\theta_0 = -\frac{k \alpha}{2I_p \Omega \omega}; \quad (17)$$

$$\varphi_0 = \frac{k \alpha}{-m_b g L + k}; \quad (18)$$

$$\omega = \sqrt{\frac{(m_b g L - k)P}{2(I_p \Omega)^2 - (m_b g L - k)(I_o + I_{gz})}}. \quad (19)$$

Equation (18) shows that the amplitude of sprung's roll regards to the torque of torsional spring. In addition to this, Equation (17) and (19) can be rearranged as

$$\Omega = -\frac{k\alpha}{2I_p\omega\theta_0}; \tag{20}$$

$$P = \omega^2 \left[ \frac{2(I_p\Omega)^2}{m_b g L - k} - I_o - I_{gz} \right]. \tag{21}$$

Figure 6 was plotted utilizing Equations (20) and (21). These above equations are used to determine the minimum flywheel speed required for a given oscillation amplitude ( $\theta_0$ ) of the gimbals. From the angular frequency scan in Figure 6, the required flywheel speed increases when operating at low frequencies. Besides, it can be deduced that as the oscillation amplitude of the gimbal increases, the required speed of the flywheel and the  $P$ -gain decrease to keep the sprung mass in balance.

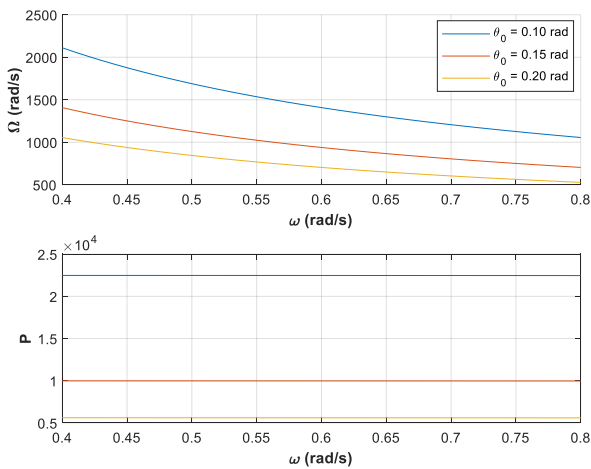


Fig. 6. Variation of flywheel speed and P-gain of the controller concerning angular frequency

#### 4. Simulations of Numerical Solutions

Lagrange’s equations are solved by using MATLAB. The properties of physical model are given in Table 1. Numerical simulations were obtained using the step size of  $0.01\text{ s}$ , and zero initials for motion. Figure 7 shows that as a function of the flywheel speed, the vehicle and gyro recover from instability after a certain angular momentum. Above the speed of  $210\text{ rad/s}$  for the flywheels on the gyroscopes placed under the vehicle, the sprung and gimbals were balanced and the oscillation amplitude gradually decreased.

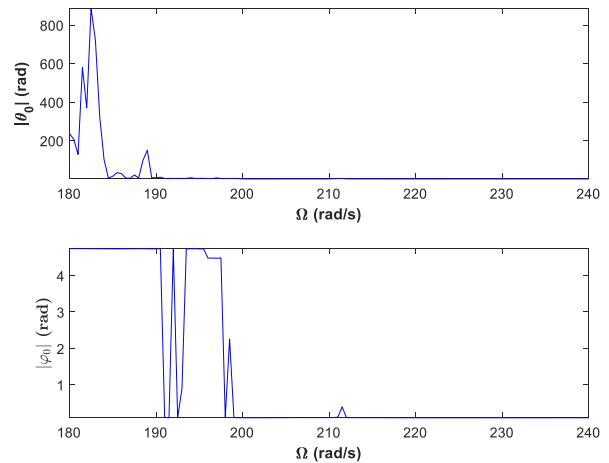


Fig. 7. The flywheel speed,  $\Omega$  scan for  $\omega = 0.5\text{ rad/s}$

If the Figure 7 obtained from Equation (21) is used to make the oscillation of the sprung at a certain frequency close to zero, the optimum selected flywheel speed is determined as  $210\text{ rad/s}$ . As can be seen from Figure 8, in order to operate at low flywheel speeds, a high frequency band should be chosen.

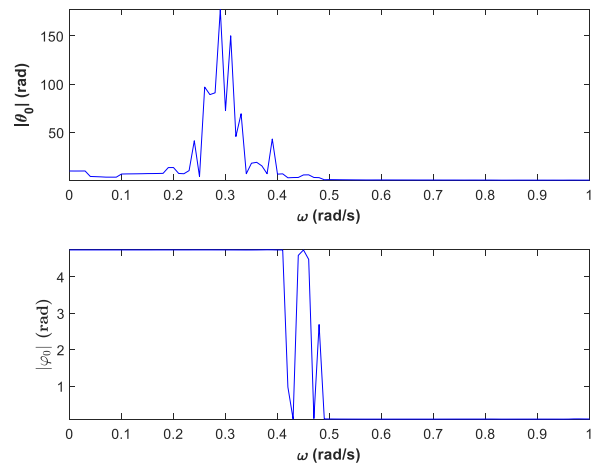


Fig. 8. The angular frequency,  $\omega$  scan for  $\Omega = 210\text{ rad/s}$

For different speeds of flywheels, figures 9 to 11 compare simulations of MATLAB (Solutions of Lagrange equations) and RecurDyn. As a result, with higher amplitude gimbal oscillations, the required flywheel speeds in the gyroscopes are lowered, so that sprung can be balanced with less angular momentum or kinetic energy. On the other hand, the stability performance of the gyroscopes can be achieved by increasing the flywheel speeds. The below comparisons agreed well with the amplitudes in Equations (17-19).

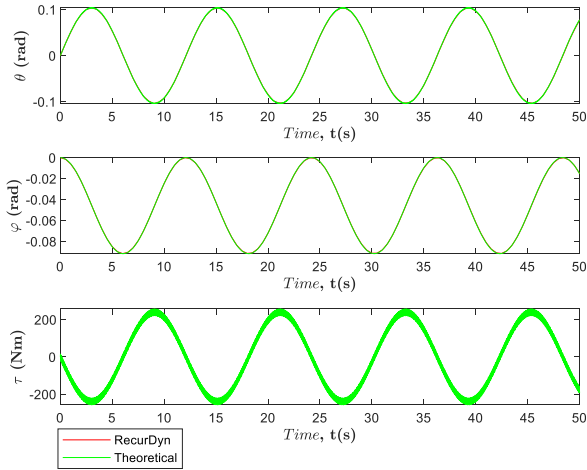


Fig. 9. Comparison of CAE software and the Lagrangian theoretical results with  $\Omega = 1689 \text{ rad/s}$ ,  $P = 22478$  and  $\omega = 0.5 \text{ rad/s}$  for  $\theta_0 = 0.10 \text{ rad}$

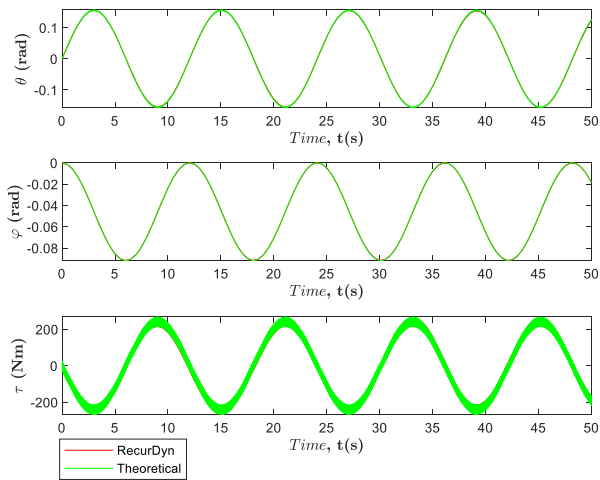


Fig. 10. Comparison of CAE software and the Lagrangian theoretical results with  $\Omega = 1126 \text{ rad/s}$ ,  $P = 9985$  and  $\omega = 0.5 \text{ rad/s}$  for  $\theta_0 = 0.15 \text{ rad}$

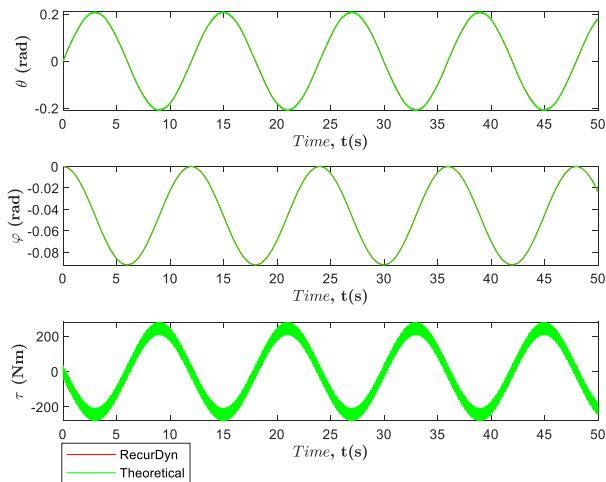


Fig. 11. Comparison of CAE software and the Lagrangian theoretical results with  $\Omega = 844 \text{ rad/s}$ ,  $P = 5613$  and  $\omega = 0.5 \text{ rad/s}$  for  $\theta_0 = 0.20 \text{ rad}$

## 5. Conclusions

It is seen that there is a correlation between P-gain and oscillation frequency at a constant flywheel speed of the gyroscope. The results of the RecurDyn simulation and the MATLAB results of the Lagrangian equations are almost the same. There is also a correlation between the flywheel speed and the precession amplitude of the gyroscope. If higher amplitude precessions are allowed, the required flywheel speeds in gyroscopes can be reduced, thereby balancing the sprung with less angular momentum or kinetic energy. However, the stability of the gyroscope should also be considered when choosing the precession amplitude of the gimbal. Because after a certain amplitude, vibrations at different frequencies come into play, affecting the stability of the gyroscope and may cause the sprung mass to rollover.

## Nomenclature

- $c$  : equivalent damping coefficient of suspensions against rotation. (N.m.s/rad)
- $D$  : vehicle's dissipation function
- $g$  : gravitational acceleration ( $\text{m/s}^2$ )
- $G$  : mass center of sprung (m)
- $I_{bx}$  : mass inertia of the sprung ( $\text{kg.m}^2$ )
- $I_{gx}, I_{gy}, I_{gz}$  : gimbal's principal moment inertia of gyroscope ( $\text{kg.m}^2$ )
- $I_o$  : flywheel's inertia of gyroscope ( $\text{kg.m}^2$ )
- $I_p$  : flywheel's rotary inertia of gyroscope ( $\text{kg.m}^2$ )
- $I_r$  : reaction wheel's rotary inertia ( $\text{kg.m}^2$ )
- $I_y$  : gimbal's mass moment inertia of reaction wheel ( $\text{kg.m}^2$ )
- $k$  : equivalent stiffness coefficient of suspensions against rotation. (N.m/rad)
- $L$  : mass centroid length of sprung (m)
- $m_b$  : mass of sprung (kg)
- $P$  : proportional gain of controller
- $T_c$  : torque exerted to gimbal as a control output (N.m)
- $T_{gyroscope}$  : each gyroscope's kinetic energy
- $T_{reaction wheel}$  : reaction wheel's kinetic energy
- $T_{sprung mass}$  : kinetic energy of the sprung
- $T_{total}$  : vehicle's total kinetic energy
- $(X, Y, Z)$  : coordinates
- $V$  : vehicle's potential energy
- $\alpha$  : road bank angle (rad)
- $\theta$  : gimbal's precession (rad)
- $\theta_0$  : gimbal's amplitude of precession (rad)
- $\tau$  : torque exerted to reaction wheel (N.m)
- $\varphi$  : sprung's roll angle (rad)
- $\varphi_0$  : amplitude of roll angle (rad)
- $\dot{\psi}$  : rotational acceleration of reaction wheel ( $\text{rad/s}^2$ )
- $\Omega$  : rotating speed of each gyroscope's flywheel (rad/s)
- $\omega$  : frequency of harmonic motion (rad/s)

### Conflict of Interest Statement

The author declares that there is no conflict of interest in the study.

### References

- [1] Ataei M, Khajepour A, Jeon S. Model predictive rollover prevention for steer-by-wire vehicles with a new rollover index. *Int J Control* [Internet]. 2020 Jan 2;93(1):140–55. Available from: <https://www.tandfonline.com/doi/full/10.1080/00207179.2018.1535198>
- [2] Jo J-S, You S-H, Joeng JY, Lee KI, Yi K. Vehicle stability control system for enhancing steerability, lateral stability, and roll stability. *Int J Automot Technol* [Internet]. 2008 Oct 7;9(5):571–6. Available from: <http://link.springer.com/10.1007/s12239-008-0067-9>
- [3] Shim T, Ghike C. Understanding the limitations of different vehicle models for roll dynamics studies. *Veh Syst Dyn* [Internet]. 2007 Mar;45(3):191–216. Available from: <http://www.tandfonline.com/doi/abs/10.1080/00423110600882449>
- [4] Reza Larimi S, Zarafshan P, Moosavian SAA. A New Stabilization Algorithm for a Two-Wheeled Mobile Robot Aided by Reaction Wheel. *J Dyn Syst Meas Control* [Internet]. 2015 Jan 1;137(1). Available from: <https://asmedigitalcollection.asme.org/dynamicsystems/article/doi/10.1115/1.4027852/473544/A-New-Stabilization-Algorithm-for-a-TwoWheeled>
- [5] Ünker F. Proportional control moment gyroscope for two-wheeled self-balancing robot. *J Vib Control* [Internet]. 2021 Apr 15;107754632110099. Available from: <http://journals.sagepub.com/doi/10.1177/10775463211009988>
- [6] Ünker F, Çuvalcı O. Optimum Tuning of a Gyroscopic Vibration Absorber for Vibration Control of a Vertical Cantilever Beam with Tip Mass. *Int J Acoust Vib* [Internet]. 2019 Jun;24(2):210–6. Available from: [http://iiav.org/ijav/content/volumes/24\\_2019\\_1848881553860721/vol\\_2/1158\\_fullpaper\\_637571561710889.pdf](http://iiav.org/ijav/content/volumes/24_2019_1848881553860721/vol_2/1158_fullpaper_637571561710889.pdf)
- [7] Ünker F. Tuned Gyro-Pendulum Stabilizer for Control of Vibrations in Structures. *Int J Acoust Vib* [Internet]. 2020 Sep 30;25(3):355–62. Available from: [https://iiav.org/ijav/content/volumes/25\\_2020\\_36521584896523/vol\\_3/1632\\_fullpaper\\_729911601404333.pdf](https://iiav.org/ijav/content/volumes/25_2020_36521584896523/vol_3/1632_fullpaper_729911601404333.pdf)